IEEE Access
Multidisciplinary | Rapid Review | Open Access Journal

Received 16 March 2024, accepted 26 March 2024, date of publication 28 March 2024, date of current version 3 April 2024.

Digital Object Identifier 10.1109/ACCESS.2024.3382757

RESEARCH ARTICLE

LEDPOS: Indoor Visible Light Positioning Based on LED as Sensor and Machine Learning

CHRISTIAN FRAGNER[1,2], CHRISTIAN KRUTZLER[1], ANDREAS PETER WEISS[1], AND ERICH LEITGEB[2], (Member, IEEE)

[1]Institute for Sensors, Photonics and Manufacturing Technologies, JOANNEUM RESEARCH Forschungsgesellschaft mbH, 7423 Pinkafeld, Austria
[2]Institute of Microwave and Photonic Engineering, Technical University Graz, 8010 Graz, Austria

Corresponding author: Christian Fragner (christian.fragner@joanneum.at)

This work was supported by Austrian Federal Ministry for Climate Action, Environment, Energy, Mobility, Innovation and Technology (BMK) within the Project 3DLiDap (Disruptive Technologies for Ultra-High-Precision 3D Light Detection and Positioning in Indoor Location-Based Services and Indoor Geofencing Applications).

ABSTRACT Accurate indoor positioning is becoming increasingly important, especially in highly automated industrial environments with robots. In addition, LED-based lighting is also being used more and more frequently in such application fields. In the present work, the possibility to exploit the LED lighting infrastructure with a novel approach for implementing an accurate indoor positioning system is investigated. For this purpose, a demonstrator luminaire LEDPOS is proposed and evaluated that combines visible light sensing based on backscattered reflections to accurately estimate the two-dimensional position of a retroreflective foil at the floor while providing simultaneously an unimpaired room illumination. In particular, the same LED elements are shared for illumination and for the sensing functionality. Furthermore, the algorithm for data evaluation and position determination is based on a machine learning approach that is implemented on the edge in the luminaire. Thus, the presented approach allows for a simple and cost-efficient implementation in different applications. The experimental characterization of the LEDPOS demonstrator in a real-world scenario shows that a very good positioning accuracy can be achieved, in which the average error for the two-dimensional position of the retroreflective foil within an area of 0.64 m^2 remains in the range of 3 cm.

INDEX TERMS Indoor positioning, LED as sensor, machine learning, visible light sensing, visible light positioning.

I. INTRODUCTION

The steady increase in LED-based lighting systems in recent years has raised a great deal of interest to investigate visible light technologies for various applications [1]. The visible part of the electromagnetic spectrum, traditionally associated only with lighting, has now emerged as a kind of revolutionary technology for communication (Visible Light Communication – VLC [2], [3]), positioning (Visible Light Positioning – VLP [4], [5], [6], [7], [8]), and sensing applications (Visible Light Sensing – VLS [9], [10]). In general, VLS systems can use variations in light intensity, color and polarization to extract valuable information about the environment [9]. This enables applications such as occupancy detection, environmental monitoring and intelligent lighting control [11], [12], [13], [14], [15], [16]. Further, VLP, representing a variant of VLS for localization purposes, can provide the basis for location-based services indoors [17], [18]. VLS and VLP can be realized by various components for the detection of light such as photodiodes or CMOS sensors. Generally less studied is the use of LEDs as sensing elements, as LEDs are primarily designed for lighting. However, due to their inherent light-emitting and light-detecting properties, LEDs can also be used as sensors and not only as light sources [19], [20], which has opened new avenues for innovation and research. This convergence of

The associate editor coordinating the review of this manuscript and approving it for publication was Jiang Wu.

lighting and sensing functions in a single device holds great potential for cost-effective and scalable solutions in the fields of sensing and positioning.

The topic of indoor positioning has also been a challenge for many years and is being addressed with various technologies aiming to provide accurate and reliable localization within enclosed spaces. The most common positioning system, the Global Navigation Satellite Systems (GNSS) [21], [22], can be weakened or even completely blocked indoors [23]. Therefore, other technologies and methods, mainly radio frequency (RF) based solutions [24], [25], Wi-Fi [26], [27], Bluetooth [28], ultra-wideband (UWB) [29], [30], ultrasound [31] and radio frequency identification (RFID) [32], [33], [34] have been investigated for indoor applications. However, these systems often have limitations in terms of accuracy, reliability and performance in complex indoor environments. In addition to these technologies, Visible Light Positioning (VLP) is another promising alternative for indoor positioning [4]. VLP is generally considered to belong to the technologies that can provide high position accuracy in the centimeter range under ideal conditions [35], [36], [37]. This property makes VLP well-suited for applications that require high-precision location, such as indoor navigation, asset tracking and location-based services. Further, VLP offers the advantage of being immune to electromagnetic interference, allowing for applications in RF-sensitive environments such as hospitals and industry. Moreover, since visible light cannot penetrate opaque media like walls, interference between different systems is reduced. Another advantage of VLP compared to RF technologies is the ability to easily shape light-beams using apertures, concentrators or lenses. This allows to confine VLP systems to certain areas within a room without disturbing the remaining space. Therefore, these general properties of light are well suited to scenarios where room level restrictions are required, allowing the implementation of independent positioning systems in each room or even multiple positioning systems in one single room [38].

Finally, as a potential part of green Internet of Things (IoT) technologies, VLP opens up opportunities for energy-efficient and sustainable indoor positioning solutions. As VLP systems can be seamlessly integrated into the existing lighting infrastructure and, in addition, also make use of the already present light sources in luminaires, cost-effective and scalable solutions become possible. Thus, the ubiquitous presence of LED lighting can be leveraged with minor need for additional infrastructure by deploying VLP systems. This also minimizes implementation costs and simplifies the adoption of this technology [39].

The remaining parts of this work are structured as follows. Section II presents the contributions, challenges and resulting design goals of this work, followed by the related work in Section III. The architecture of the proposed LEDPOS system, the hardware and measurement algorithm, as well as the experimental setup for evaluation are described in Section IV. The selection and implementation of the two-dimensional positioning algorithm is discussed in Section V and the evaluation of measurement results is provided in Section VI. A discussion and outlook on future work is given in Section VII. Finally, the conclusion is drawn in Section VIII.

II. CONTRIBUTIONS, CHALLENGES AND DESIGN GOALS

In this work, a novel LEDPOS demonstrator luminaire is investigated that is capable of accurately determining the two-dimensional position of a retroreflective foil by evaluating the backscattered light while simultaneously providing unimpaired room illumination. It is important to note that the system does not require any additional light sensitive device such as a photodiode or camera. Instead, the LEDs of the luminaire are switched alternately between illumination and sensing modes at a frequency that is kept beyond the limits perceived by the human eye, thus maintaining a flicker-free lighting quality. In addition, all data processing and the machine learning classification algorithm for actual position determination of the retroreflective foil is computed on the edge in the luminaire. The combination of lighting and sensing functionalities as well as the practical implementation of these features into a system for a real-world scenario poses a number of challenges, which are discussed below. First, the contributions of this work are summarized as follows:

- The electronic design for the development of the proposed LEDPOS demonstrator luminaire is presented. In essence, this contains a circuit design that enables the simultaneous measurement of reflected light and illumination by LEDs.
- The developed measurement method for processing LED sensor data, to enable two-dimensional positioning estimation by machine learning, is described with its target feature for edge computing.
- In detail to the previous item, the selection and implementation of an appropriate supervised machine learning based algorithm to predict the two-dimensional position of a retroreflective foil is given.
- The experimental setup to finally verify and validate the proposed LEDPOS demonstrator luminaire in a real-world environment is presented.

The challenges of using an LED as a sensor and the implementation of a two-dimensional positioning algorithm on the edge in a luminaire are discussed in the following subsections.

A. CHALLENGES OF USING LED AS A SENSOR

Due to the physical similarity of the pn-junction of a photodiode and an LED, it is possible to use the photoelectric effect to operate an LED as a receiver. However, LEDs are generally not designed to be used as photodiodes and therefore, their sensitivity and bandwidth are much lower than those of photodiode detectors. For sensing applications, a high signal-to-noise ratio (SNR) is crucial, particularly when very weak or attenuated signals are to be detected, as is

the case with an LED as sensor [40]. The sensitivity spectrum of an LED is also a property relevant for sensing purposes. When used as a photodiode, an LED is only sensitive to incident photons of the same or a smaller wavelength than that of its own emission, due to the bandgap structure of different semiconductor materials [41]. Another issue associated with LEDs is their sensitivity to temperature variations, which can affect their sensory performance and accuracy [42]. Usually, temperature changes alter the electrical and optical properties of the LED, resulting in variations of the detected signals. Regarding applications with combined illumination and sensing purposes, cross-talk and interference can also significantly affect the performance of LEDs as sensors. Crosstalk refers to the unwanted coupling of the light emitted from the LED with detection, leading to interference and inaccurate measurements. Last but not least, in contrast to other publications using LEDs as a sensor (e.g. [43]) a major challenge is to use the same LEDs as sensor as well as for flicker-free illumination. The combination of these functionalities further increases the complexity to accurately measure the reflected light, as switching between these modes generates higher temperature variations and thus additional noise.

B. CHALLENGES OF MACHINE LEARNING ALGORITHMS FOR EDGE COMPUTING

Microcontrollers are commonly engaged for edge computing, but typically have limited computational resources in terms of processing power, memory and storage capacity. Thus, the implementation of complex machine learning algorithms on microcontrollers can be challenging due to resource constraints [44]. First, limited memory capacity may restrict the size and complexity of models that can be deployed on microcontrollers. Secondly, the selection of an appropriate algorithm is crucial, because algorithms differ significantly in their computational power and memory size requirements. Therefore, the adaption of existing algorithms by optimizing them for low-power or low-memory operation poses a challenge to work efficiently for edge computing on microcontrollers. Data acquisition, preprocessing and, for example, feature extraction techniques need to be carefully designed to cope with limited resources [45].

C. DESIGN GOALS

The design goals for the LEDPOS demonstrator and its evaluation are defined based on the challenges described above and to meet the overall objectives of this work:

1) **Accurate measurement of backscattered reflections using white LEDs as a sensor:** High sensitivity is essential to accurately detect and measure even weak backscattered reflections where the resulting photocurrent can be in the small nanoampere range. To this end, two points are of major importance. First, the selection of a proper LED is crucial. On the one hand, it is well known that the sensitivity of white LEDs in particular is poor compared to colored ones [46]. On the other hand, since the LEDPOS demonstrator is designed for a real-world application, illumination with white LEDs is an integral part of the system requirements. Therefore, a white LED capable of capturing a wide range of reflections and low intensities needs to be selected to allow for accurate measurements in different scenarios. Secondly, the design of the transimpedance amplifier (TIA), which is connected to the sensing LED and responsible to convert the resulting photocurrent into a proportional voltage, is crucial in terms of the detectable range, bandwidth and hence the overall accuracy of the system.
2) **Noise and temperature optimized hardware design:** In close relation to the previous design goal, the second target for the hardware design is to minimize noise throughout the electronic printed circuit board (PCB). Noise can degrade the performance of electronic circuits and thus affect the accuracy of measurements or signal processing. Therefore, layout, grounding and shielding techniques should be carefully considered to minimize noise sources and ensure clean signal paths. In addition, the selection of components with low noise characteristics and the implementation of appropriate filtering mechanisms are also essential to reduce noise in the system. Another important design consideration is optimization with regard to temperature effects. Temperature variations can have a significant impact on the performance and reliability of electronic circuits, especially when it comes to LEDs. Therefore, the design should focus on thermal management techniques to ensure stable operation over time.
3) **Deployment of a supervised machine learning based positioning algorithm on a microcontroller:** From the multitude of available machine learning algorithms, approaches to create a model for position determination based on labelled training data (supervised methods) are investigated. The algorithm finally selected should provide high positioning accuracy to map new input features to the corresponding two-dimensional position while taking into account the typical constraints for edge computing on a microcontroller in terms of computational resources including processing power, memory and storage capacity. The performance of the algorithms considered is compared and evaluated using metrics such as localization accuracy, distance differences and error metrics to ensure reliable and accurate positioning results. Further, the algorithms need to be optimized regarding complexity, memory requirements and efficient data structures for efficient deployment on a microcontroller.
4) **A scalable, real-world experimental setup for a reproducible evaluation of the LEDPOS demonstrator system:** The experimental test setup and test environment for an evaluation of the LEDPOS system

should support adjustable positions of a retroreflective foil on the floor below the ceiling-mounted LEDPOS system to analyze the performance of the system for position determination under various scenarios and configurations of reflected light. The use of a retroreflective foil is mandatory to reduce the impact of additional reflections from the environment. In addition, a retroreflective foil is readily available, low-cost and can be attached to various devices, such as a robot. Further, the setup must provide reproducible data collection in terms of repeated conditions and positions and should also be adaptable to different ambient light conditions.

In summery, the LEDPOS demonstrator presented in this work contributes significantly to the advancement of backscattered based indoor visible light positioning with its realization addressing the outlined challenges. The main advantage and contribution is that no additional photodiodes or CMOS sensors need to be utilized, since the LEDs themselves are used as both light sources and sensors. Consequently, in terms of energy efficiency and sustainability, the approach presented here of using LEDs as sensors offers unprecedented opportunities for retrofitting, as only LEDs are used, identical to existing lighting, and no space is required for additional photosensitive devices.

III. RELATED WORK

The related work in the field of using LEDs as sensors in general and for the application of VLP in particular is reviewed in the following subsections.

A. LED AS SENSOR

The basic use of an LED as a photosensitive device was confirmed more than 20 years ago [19], [20]. At present, research is increasingly focusing on the use of LEDs as transceivers, especially in the field of VLC, with an emphasis on basic communication properties such as transmission speed, distance and error rate. To improve these target properties, the selection of a suitable LED for transmission and reception of light is paramount. The photodetector characteristics of different colored low-power LEDs available on the market were analyzed and methods for measuring the response sensitivity and bandwidth demonstrated [46]. It was found that the response sensitivity and bandwidth can be improved by increasing the reverse bias voltage on the LED. Furthermore, LEDs in the higher visible wavelength range (yellow, orange, red) showed significantly better properties compared to the lower wavelength spectrum (blue, green). The white LED tested showed no photosensitive properties at all. Commercially available high-power SMD LEDs were investigated in [47] and the results showed good photosensitive properties compared to low-power LEDs, but also to photodiodes. Again, the yellow, orange and red LEDs gave the best results in terms of sensitivity. In [48], low-power RGB LEDs were tested for their transmitter and receiver characteristics. It was found that a combination of the green LED chip as emitter and the red LED chip as receiver gave the best results for the measurement distance of 3 cm. In [49], LED-LED communication with a transmission rate of 100 Mbit/s was demonstrated using low-power LEDs (red and orange) over a distance of a few centimeters. On the receiver side, a TIA was used in combination with a digital equalizer to avoid bandwidth limitations. Similarly, the capability of yellow LEDs as receivers for communication speeds above 3 Gbit/s was demonstrated at a distance of 2 m with a green laser diode for transmission [50]. A multi-input multi-output (MIMO) VLC system for half-/full-duplex communication was demonstrated using RGB LEDs at a transmission rate of 40 or 20 kbps and a distance of 10 cm [51].

As already stated before, the extremely low photocurrents pose a major challenge when using LEDs as sensors. Thus, an alternative method for measuring the photocurrent of an LED was presented based on the correlation between the magnitude of the photocurrent and the discharge time of the LED capacitance [52] and [53]. In [54], a LED sensor device was investigated for colorimetric analysis, and in [55], [56] similar configurations were tested for colorimetric flow analysis, pH as well as phosphate determination. However, in all this works, two separate LEDs were used for sensing and illumination. The application of LEDs for a miniaturized spectrometer device was studied in [57], with the LED components acting as detectors in different wavelength ranges. Finally, a single RGB LED (Cree XLamp MC-E Color) was investigated for simultaneous color sensing and LED control [58], but in fact there is rather limited published work on the application of LEDs as sensors. In [59], RGB LEDs are used for multiple tasks, such as communication, energy harvesting and sensing. For the sensing scenario, the detection of sunlight and the detection of wavelength variations to sense the health of a plant are demonstrated. However, for the sensing scenarios, the RGB LEDs are not switched between sensing and illuminating, which challenges the use of an LED as a sensor instead of a photodiode.

One more study is to be mentioned that investigates occupancy determination in a 30 m^2 office setting and uses the LED lighting infrastructure for illumination and sensing. Contrary to the approach presented in this work, arrays of LEDs are used to overcome the problem of sensing the extremely small photocurrents caused by the reflectance variations of the occupants in the room, and second, the evaluation algorithm for signal analysis runs on an external server [43]. Thirdly and most importantly, in [43] the LEDs are switched between illumination and sensing every 10 minutes, whereas in this work the LEDs are switched at frequencies above the perception threshold of the human eye, making the dual use of the LEDs truly undetectable to a human observer. In [60], the testbed shown in [43] was used to demonstrate improved occupancy detection based on LED lighting using Bayes filters and neural network classification, especially in dynamic and regular patterns.

B. VISIBLE LIGHT POSITIONING

As discussed in the introduction, Visible Light Positioning (VLP) has emerged as a promising technology for indoor positioning and localization, taking advantage of the widespread deployment of LED lighting infrastructure. VLP systems can use different methods and techniques to estimate the position of a receiver or an object in an indoor environment. This section provides an overview of the different methods used in VLP, including geometry-based methods, Angle of Arrival (AoA), Received Signal Strength (RSS), Time of Arrival (ToA), Time Difference of Arrival (TDoA), proximity-based methods and fingerprinting. In addition, the differences between device-free and device-based VLP systems are discussed in the context of the green Internet of Things (IoT). Recent reviews on these topics can be found, e.g., in [8], [35], [36], [37], [61], [62], and [63].

Geometry-based methods in VLP rely on the geometric relationship between the transmitters (LEDs) and the receiver to estimate the receiver's position. These methods use the known locations of the LEDs and measure the distances or angles between the receiver and multiple LEDs to determine the position (see, for example, [64], [65] for implementation examples). Geometry-based methods provide accurate positioning when the geometry of the environment is well defined, but are sensitive to errors in distance or angle measurements. The receivers used in these methods are commonly based on photodiodes, cameras or photomultipliers [66] that provide data such as angles for the incident light or the light intensity for position calculation [4], [67]. AoA estimation is a widely used technique in VLP systems [68]. It involves capturing the incoming light signals from the LED transmitters and estimating the angles of arrival to determine the position of the receiver. Hong et al. [69] showed an AoA based VLP system using quadrant-solar-cell and third-order ridge regression machine learning with an resulting average position error of 3.09 cm.

RSS can also be used as a parameter in VLP systems to estimate the position of a receiver. The receiver measures the strength of the received light signals from several LED transmitters. Then RSS-based methods estimate the receiver's position based on the received power, taking into account signal attenuation due to the distances between the receiver and the transmitters [68]. RSS measurements can be susceptible to environmental factors such as signal attenuation, reflections and interference. However, with proper calibration and signal processing techniques, RSS-based VLP systems have shown promising results in terms of accuracy and cost-effectiveness [70]. In [71], a RSS-based VLP system is shown with simulation results indicating a positioning accuracy in the low double-digit centimeter range.

Time-based methods, including ToA and TDoA, rely on precise time measurements to estimate the position of the receiver. ToA-based VLP systems measure the time it takes for light signals to travel from the LEDs to the receiver and calculate the corresponding distances [4], [68]. TDoA-based VLP systems use differences in signal arrival times from multiple LEDs to estimate position and require synchronized clocks between the LEDs and the receiver. However, the enormous speed of light in combination with the rather small distances pose a challenge for accurate ToA and TDoA measurements. The high precision of clock synchronization required for these measurements makes these approaches impractical for VLP [39]. Consequently, ToA is commonly used in ultrasound-based systems where signals travel at a comparatively slower rate, but remains unexplored for an implementation in VLP [38]. In [72], a 3D ToA localization approach using sound waves is elaborated, which allows positioning accuracy between 10 cm and 20 cm.

Fingerprinting is another popular approach for VLP that uses a database of pre-collected signal measurements to estimate the position of the receiver. The receiver measures the signal characteristics of the LEDs and compares them with the training database. The position is then estimated based on the closest matching fingerprints. Fingerprinting-based VLP systems can achieve high accuracy in complex indoor environments with a sufficient number of reference measurements. However, maintaining and updating the fingerprint database can be challenging in dynamic environments. In [73], a fingerprinting VLP system based on RSS using a weighted k-nearest neighbors algorithm approach is proposed. The experiments showed an average positioning error of 3.04 cm in an area of approximately 9 m^2. Recently, also different machine learning algorithms were investigated in combination with simulations to reduce the fingerprinting database for VLP with a photodiode receiver in a real-world scenario. Besides the need for an active receiver in this approach, the localization algorithm was implemented on a 2.6 GHz CPU with 8 GB RAM [74].

Another differentiation commonly discussed in the literature pertains to the configurations of VLP systems, namely device-based and device-free configurations. Device-free systems do not require specialized receiver equipment at the object of interest [37]. Instead, they simply rely on detecting variations in the received light signal caused by the movement or presence of objects in the environment. This can be achieved through changes in RSS, AoA or other measurable parameters. Device-free VLP has attracted interest for applications such as occupancy detection, tracking, and context-aware services. By leveraging existing lighting infrastructure and avoiding the need for dedicated receivers at objects of interest, device-free VLP systems offer cost-effective and scalable solutions for indoor positioning. Sometimes such device-free configurations are also referred to as Backscattered VLP (BVLP) and studies conducted for such setups range from receivers in the ceiling light [75], receivers on the walls [76], to receivers integrated into the floor [77]. In [78], a device-free VLP system is presented which achieved median errors of 0.68 m, 1.20 m and 0.84 m depending on the test environment. Contrary to device-free configurations, device-based VLP systems use specialized receiver devices such as photodiodes, cameras or photomultipliers at the

object of interest to capture and process the light signals for accurate positioning. In general, these systems provide greater control over the received signals, enabling higher accuracy and more advanced localization techniques.

IV. LEDPOS DEMONSTRATOR AND METHODS

This section presents the system architecture and hardware design of the LEDPOS demonstrator with its key properties. These include the use of standard white-light LED components and a microcontroller to realize a scalable VLP system for a real-world scenario, based solely on the backscattered reflections from a passive retroreflective foil and requiring no further active components on an object of interest. Thus, this approach is considered to comply with device-free and BVLP configurations as discussed in Section III. Further on, the method for the combined illumination and sensing functionality is described and finally the experimental setup for the evaluation of the LEDPOS demonstrator for VLP is shown on an area of 1.44 m^2 on the floor below the ceiling mounted demonstrator. Please note that in the evaluation of the results (see Section VI) the total area of 1.44 m^2 (1.2 m $\times$ 1.2 m) is further divided into subsets of 0.64 m^2 (0.8 m $\times$ 0.8 m) and 0.16 m^2 (0.4 m $\times$ 0.4 m). It is to be mentioned here that initial investigations on this approach were already presented in [79] and that the current work is based on these studies. However, the LED sensing capability is significantly improved by the new hardware design presented as well as the algorithm, allowing for increased position accuracy and a system that is scalable for real-world environments.

A. SYSTEM ARCHITECTURE

An overview of the system architecture and its main functionality is given in Fig. 1. The demonstrator system consists of one luminaire containing four white-light LEDs that are additionally equipped with reflectors with a 20° beam angle. The parallel illumination and sensing tasks are realized by three LEDs for lighting and one LED for concurrent detection. The steps for data acquisition and position determination by machine learning algorithms on the implemented microcontroller are indicated in the flowchart of Fig. 1 at the right. Consequently, the LEDPOS demonstrator provides an approach for implementing an autonomous VLP system into the existing lighting infrastructure. Notably, this approach does not require any additional photosensitive components.

B. LEDPOS HARDWARE

The concept for illumination and sensing tasks in parallel is based on four controllable white LEDs (Cree XLamp MC-E White 4000K) that are perpetually toggled between light emission and light sensing states. Therefore, each LED has its own transceiver circuit that handles these illumination and sensing intervals. In the following, the main parts of the demonstrated luminaire hardware are described in detail. A representation of the finally assembled PCB is provided in Fig. 2a and 2b. The corresponding block diagram is shown in Fig. 2c, where each block is mapped to its corresponding position on the assembled board. It contains four identical transceiver circuits with corresponding LEDs and PWM drivers as well as the TIA stages and the microcontroller board is attached to the bottom side of the developed PCB.

The entire hardware of the luminaire is supplied externally with 12 V DC from a laboratory power supply. To ensure a stable and undisturbed voltage, protection and filtering circuits are implemented in the supply section of the PCB. Further, a linear voltage regulation circuit is used for the 3.3 V supply of the microcontroller unit and the TIA stages.

1) TRANSCEIVER UNIT

Each of the four equivalent designed transceiver unit circuits consists of a white LED, switching components, and a transimpedance amplifier circuit followed by an analog-digital converter (ADC). In general, the transceiver unit is responsible for alternately switching the corresponding LED to a zero-biased state (light receiving mode) and a forward-biased state (light emitting mode), see Fig. 3a showing the current flows during the zero-biased state in red and the forward-biased state in blue.

In the zero-biased state, the n-channel metal-oxide semiconductor (nMOS) transistor Q1 is open, while the second nMOS transistor Q2 is conducting. Thus, the anode of the LED and the LED driver output are connected to ground, while the cathode of the LED is connected to the TIA input. During this phase, incident photons at the LED generate a photocurrent, which is converted into a proportional voltage by the TIA stage. Due to the fact that the photocurrent is in the nA to μA range, a two-staged TIA design is applied. It is therefore also important that the amplifier's input bias current is as low as possible, which has been taken into account in the selection of the operational amplifier. In order to reduce the noise level caused by the buck converter, a first order low-pass filter with a cutoff frequency below the switching frequency of the LED buck driver (400 kHz) is added between the first and the second TIA stage. Finally, the voltage output of the second TIA stage is acquired by an ADC pin of the microcontroller unit.

In the forward-biased state, exactly opposite to the zero-biased state, the nMOS transistor Q1 is conducting, while the second nMOS transistor Q2 is open. Here, the cathode of the LED is connected to ground potential, while the anode of the LED is connected to the LED driver output. This results in a current flow from the driver through the LED and operates the LED in the direction of illumination.

Each nMOS transistor is driven by a pulse-width modulation (PWM) pin of the microcontroller unit connected to the gate of the transistor, i.e. a high level at the gate results in current flow between the drain and source (transistor is closed). Conversely, a low level at the gate results in a high resistance in the drain-source path (transistor is open). Typically, both transistors Q1 and Q2 are driven by the same PMW signal to enable the sensing and emitting functionality, but naturally with an inverter put in front of

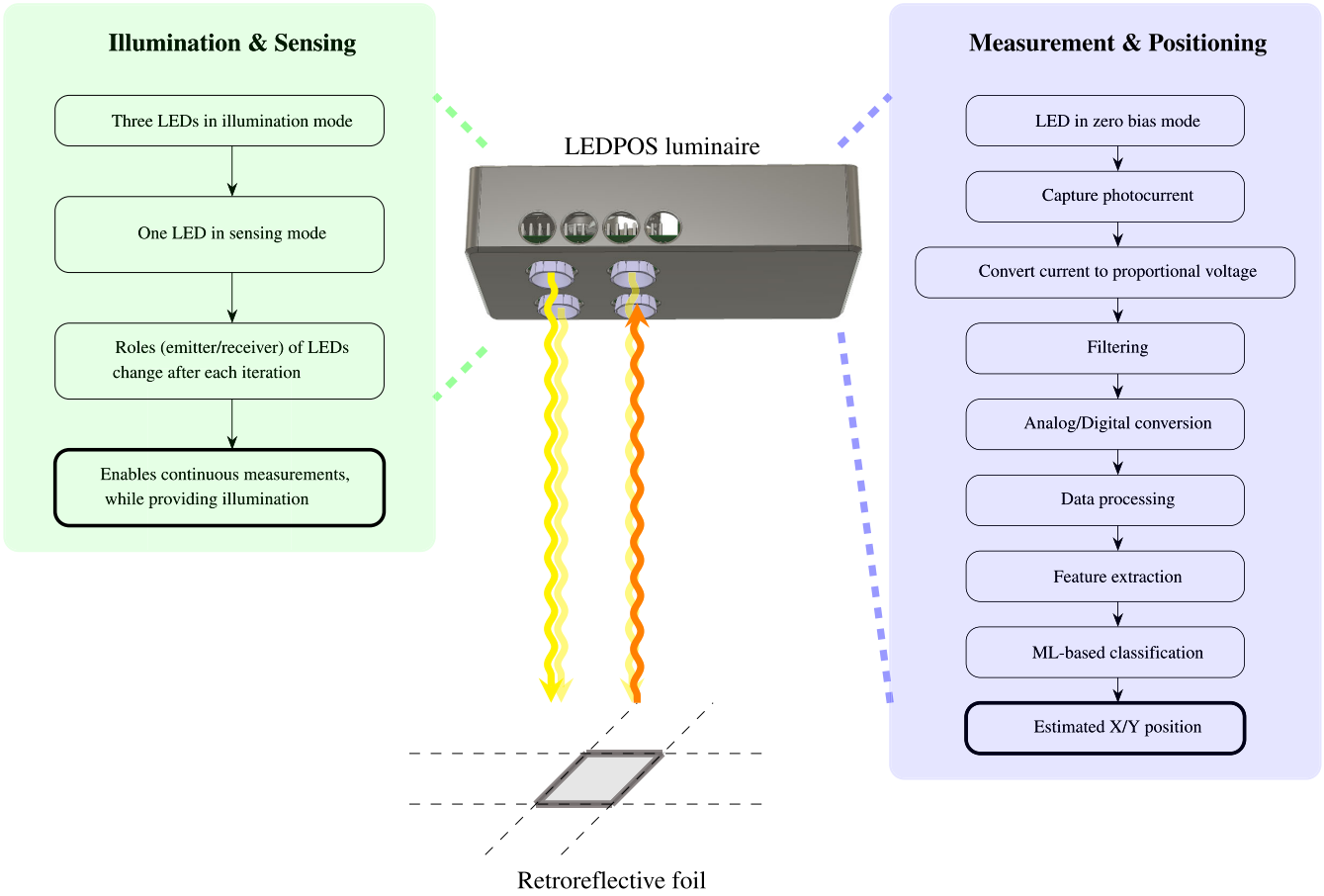

FIGURE 1. LEDPOS system architecture and schematic setup for evaluation. The LEDPOS luminaire is mounted on the ceiling and the retroreflective foil at the floor can be positioned in an area of 1.2 m × 1.2 m.

Q2. Simultaneously, the LED driver is controlled by the same PWM signal as the transistor Q1, which ensures that Q1 is closed (PWM signal high) when the LED driver is active for illumination. Due to the fact, that the PWM signal for the LED driver is almost in phase for Q1 and Q2 (Q2 inverted), it was observed that the simultaneous switching of both transistors can cause a short circuit current if both transistors are closed during their transition time. This can occur in the range of picoseconds to nanoseconds and results in an undefined behavior at the input of the TIA stage causing a higher noise level at the ADC input. Therefore, to ensure a reliable and noise reduced operation, a certain period of time is waited between the closing of one transistor and the opening of the other transistor. This time period is usually referred to as dead-time in the PWM settings, see Fig. 3a.

2) LED DRIVER

The LED buck driver circuit to maintain a constant current incorporates a step-down converter IC together with passive components such as inductors, resistors, capacitors, and diodes. When power is supplied to the step-down driver circuit (4.5 V to 32 V input supply range), the switching transistors rapidly turns on and off at a high frequency. Energy is stored in the inductor during the on-states, and the stored energy is released to the LED during the off-states. By controlling the switching frequency and duty cycle, the buck driver adjusts the average current through the LED to maintain the desired constant value. The implemented nMOS design has an internal switching frequency of 400 kHz and is able to provide a maximum LED current of 2 A. It should be noted that switching the buck driver at this high-frequency can generate electromagnetic interference (EMI). Therefore, to reduce the EMI as well as damp voltage spikes and transients within the LED buck driver switching circuit, additional EMI filters, ferrite beads and a RC snubber are used in the LED driver circuitry.

3) MICROCONTROLLER UNIT

The hardware of the proposed LEDPOS luminaire is driven by a STM32 Nucleo-G474 microcontroller board mounted on the bottom side of the PCB, see Fig. 2b. The STM32-G474RE microcontroller is a member of the STM32G4 family developed by STMicroelectronics. Based on the Arm Cortex-M4 core, the microcontroller operates at a maximum frequency of 170 MHz and offers a wide range of peripherals and interfaces. It further provides 512 kB of flash memory

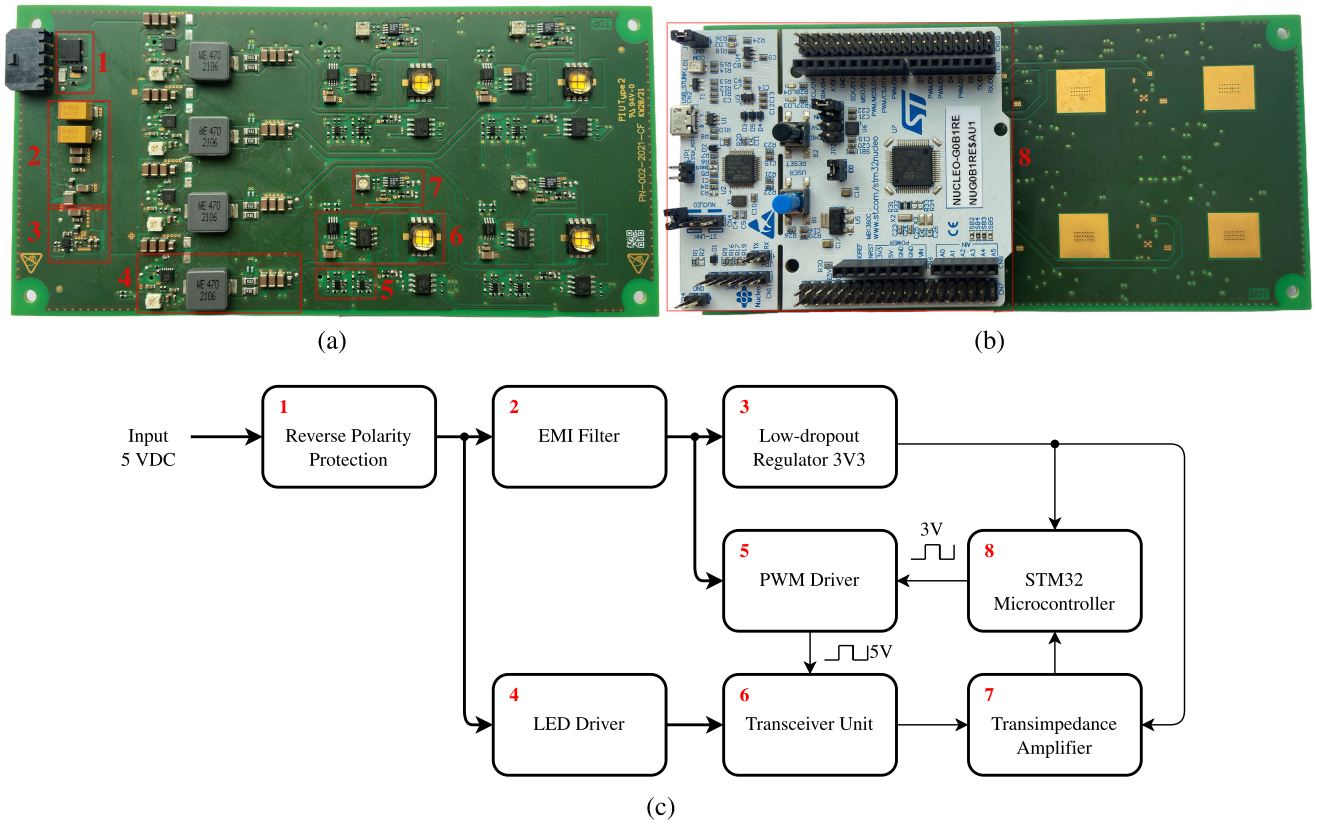

FIGURE 2. Image of the assembled LEDPOS hardware board with its functional blocks. (a) PCB top view with four transceiver circuits, (b) bottom view with a microcontroller attached to the PCB, and (c) corresponding block diagram of the LEDPOS hardware. The red numbers labelling each block are also indicated in (a) and (b).

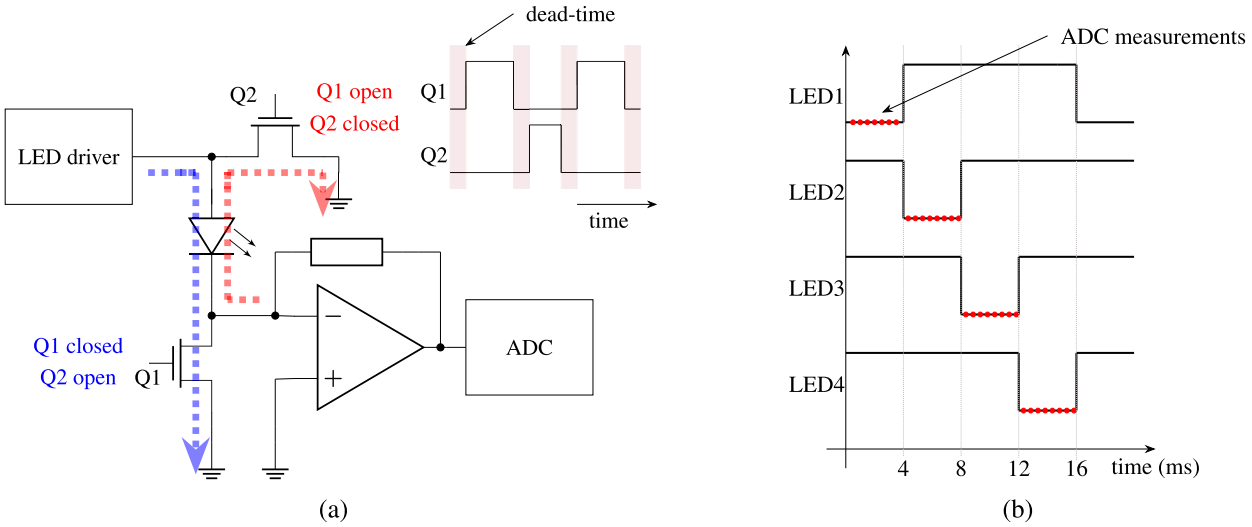

FIGURE 3. LEDPOS transceiver unit for simultaneous illumination and measurement of the backscattered light. (a) Schematic circuit of one transceiver unit indicating the light receiving mode in red and the light emitting mode in blue. (b) Measurement concept for the four transceiver units. The points in red indicate the consecutive measurement modes of each transceiver unit over time.

and 128 kB of random-access memory (RAM). It also includes a comprehensive set of communication interfaces, including multiple USART, SPI, I2C and CAN interfaces, which enable a seamless connectivity to external devices and systems. The main reason for choosing this microcontroller was the comprehensive set of analogue peripherals, such as 12-bit ADCs, DACs and comparators, which allow precise analogue measurements of the TIA stages output. In addition, this controller includes a single-precision floating-point unit (FPU) capable of accelerating floating point operations,

which are further on used in processing of the algorithm for positioning.

C. MEASUREMENT CONCEPT

For simultaneous illumination and measurement of the reflected light which is backscattered from the retroreflective foil, a concept is applied, where the four transceiver units of the LEDPOS hardware are either in illumination mode (LED forward-biased) or in measurement mode (LED zero-biased). This concept has already been introduced in [13] and [79]. To provide sufficient illumination, three of the four transceivers always are in illumination mode, while one transceiver LED is in measurement mode for capturing the reflected light. After measuring at one LED, the transceiver modes are switched and the next LED is employed for sensing. Thus, a total of four measurement intervals at each of the four LEDs are required to obtain one dataset or one cycle from all four transceiver units. This concept is illustrated in Fig. 3b. The duration of sensing at one LED is set to 4 ms and therefore, complete datasets or cycles containing the readings from all four transceivers units are available every 16 ms. The ADC acquires the data for a duration of 2 ms within each 4 ms interval (see the PWM dead-time issue discussed above) at a sample rate of 500 kS/s. Finally, the resulting 1000 samples for each measurement interval of 2 ms are averaged, to obtain their arithmetic mean. Thus, a dataset of one measurement cycle contains four means which are related to the detected light intensities at each of the four LEDs as an input to the position determination algorithm (see Section V).

Finally, it should be pointed out that the proposed measurement principle, together with the design of the demonstrator setup eliminates crosstalk, as the light from the three transmission LEDs cannot affect the fourth sensing LED.

D. EXPERIMENTAL SETUP

The experimental setup for system evaluation consists of the proposed LEDPOS demonstrator, a quadratic-shaped retroreflective foil of 10 cm × 10 cm and a two-dimensional linear axis for reproducible positioning of the foil at the floor below the LEDPOS demonstrator luminaire. The luminaire contains the hardware PCB in a 3D printed housing and is mounted on the ceiling of a laboratory rail system at a height of 2.7 m above the floor. The retroreflective foil (3M^{TM} Diamond Grade^{TM} 4090) is attached to the two-dimensional linear axis, which is fixed to the laboratory floor, see Fig. 4 for an image of this setup. The accessible experimental area underneath the luminaire is elaborated by light simulations, showing that a size of 1.2 m × 1.2 m is illuminated at the floor. Note that the luminaire is positioned in the center of this area and the emitted illuminance was measured with a mobile spectrometer to be 82 lx. The result of the illuminance simulation for the test area using the ReluxDesktop simulation software [80] and the given hardware configuration is shown in Fig. 5. The two-dimensional position of the retroreflective foil is controlled and monitored by a Python script and an USB connection to a computer. For visualization, training and testing purposes, the microcontroller unit of the luminaire is also connected to a computer via USB. All together this setup allows simultaneous control of the linear axis, while the measurement data are transmitted to a computer for a given position of the retroreflective foil.

V. TWO-DIMENSIONAL POSITIONING ALGORITHM

This section describes the two-dimensional position determination of the retroreflective foil by the LEDPOS demonstrator. First, the data processing of the captured reflections and the feature extraction are outlined. Then, in order to predict the position, a comparison of different supervised learning algorithms is performed to find an optimized solution in terms of position accuracy and the available resources of the chosen microcontroller. Finally, the training of the model and its implementation on the microcontroller are described.

A. PREPROCESSING AND FEATURE EXTRACTION

As outlined in Section IV-C, four mean values related to the detected light intensities at each of the four LEDs are provided as a dataset of one measurement cycle for position determination. To further reduce the effects of peaks due to disturbances and noise, a moving average algorithm is used for preprocessing these four means. Thus, moving average ADC values are then obtained for each LED after each measurement cycle of 16 ms, which are used as the basis for feature extraction and as the input to the machine learning algorithms.

At first the goal for position determination is defined by specifying a step size of 5 cm in x- and y-axis directions for the possible positions of the retroreflective foil in the total test area of 1.2 m × 1.2 m. This gives 625 possible positions (output labels) for the foil at the floor which by far exceeds the number of possibilities in our previous work [79]. Due to the fact, that the model of the supervised learning algorithm is computed and stored on the microcontroller, memory consumption, processing speed and other parameters must be taken into account for feature selection in view of this large number of output levels. However, the selection of meaningful features is a crucial step to construct an accurate supervised learning model. Consequently, several possible features such as the ratio, the difference, the correlation and other metrics between the four moving average ADC values of the respective transceiver units, were analyzed and finally four features selected. These selected features, which were found to give the best performance, are basically rescaled moving average values of the four transceiver measurements by mapping the moving average values to a range from 0 to 65535 and represented by a 16-bit integer, with the minimum and maximum sensor values automatically determined with each measurement cycle.

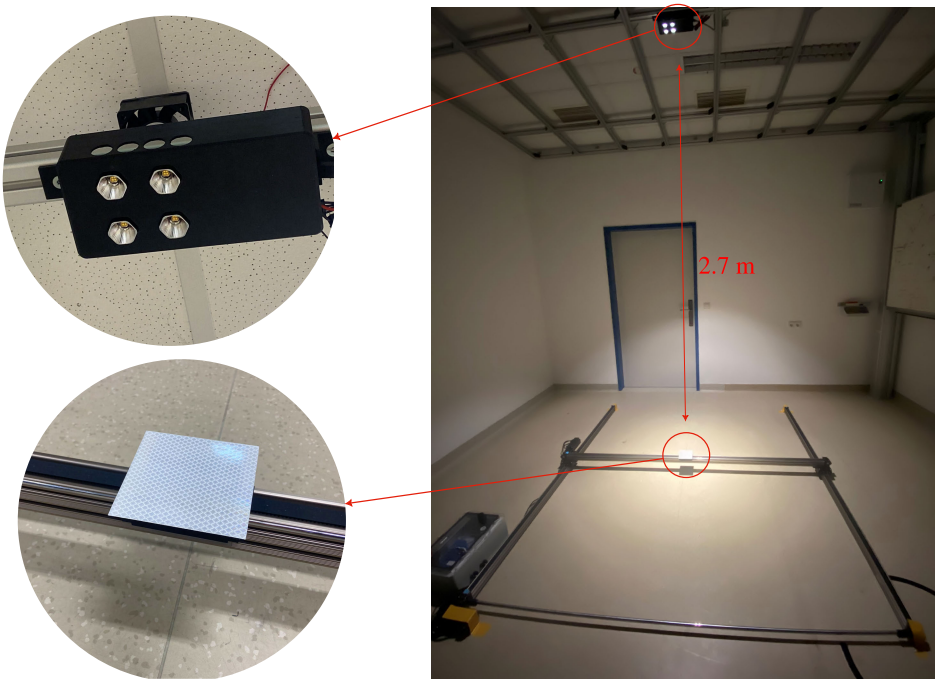

FIGURE 4. Image of the measurement setup in a laboratory room for evaluation of the LEDPOS demonstrator. The ceiling mounted LEDPOS hardware and the retroreflective foil at the two-dimensional linear stage are shown in the insets.

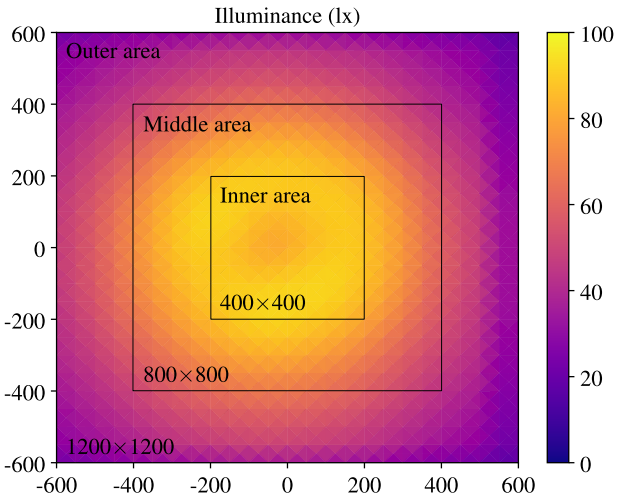

FIGURE 5. Illuminance simulation of the experimental area at the floor (axis dimensions are given in mm).

B. TRAINING DATASET GENERATION

The generation of a training dataset involves the collection, transmission and processing of data, which are obtained from the experimental setup. This training dataset is used then for the creation of machine learning models with various machine learning algorithms to finally select a suitable algorithm for positioning.

The training dataset is generated by collecting the LED sensor data as described in Section V-A and by labelling these measurements with the known position data from the 2D linear axis (see Section IV-D). Thus, the resulting training dataset consists of 5 columns containing 4 features and 1 label which is the actual two-dimensional position of the foil. For the generation of the training data, as well as for further test runs, the step size of 5 cm is used in the area of 1.2 m × 1.2 m. For each of the 625 possible positions of the retroreflective foil, 100 readings are taken for each feature at 100 ms intervals resulting in a training dataset with 62500 rows. In total, 3 such datasets were created and feature values averaged to cancel out inaccuracies as for example caused by small position deviations of the 2D linear stage. Furthermore, such training datasets were generated first in the absence of ambient light, i.e. with the room lighting switched off and the blinds closed (“without ambient light”), and second, with the fluorescent room lights in the laboratory switched on but blinds still closed (“with ambient light”).

C. SELECTION OF A SUPERVISED LEARNING ALGORITHM

In general, implementations of the most common supervised learning algorithms in microcontroller spaces are well tested, see for example [45]. However, the computational limitations of the selected microcontroller in terms of limited memory and processing power need to be taken into account to ensure an efficient and effective deployment of machine learning models.

Typically, training-based VLP algorithms rely on machine-learning techniques [81], [82] such as Support Vector Machine (SVM) [83], Random Forest (RF) [84], K-Nearest Neighbor (k-NN) [85] and Artificial Neural Network (ANN)

TABLE 1. Comparision of different supervised learning algorithms according to selected performance metrics for two sizes *n* of gererated training datasets.

Algorithm	MAE		RMSE		CA	Mean Error Distance	n
	x	y	x	y			
k-Nearest Neighbours	0.581	0.156	15.225	3.549	99.82%	0.615 mm	62500
	8.963	3.095	59.106	35.495	97.62%	10.303 mm	6250
Random Forest	0.488	0.208	13.311	4.427	99.91%	0.577 mm	62500
	9.467	3.311	75.594	36.445	98.12%	10.629 mm	6250
Decision Tree	1.64	0.76	30.258	19.12	99.82%	2.039 mm	62500
	18.682	11.987	91.788	82.546	98.15%	25.43 mm	6250
Neural Network	31.87	13.58	127.74	61.52	80.03%	38.12 mm	62500
	63.13	25.37	179.63	88.26	64.23%	75.59 mm	6250

[86]. For the selection of a suitable algorithm in this work, several promising algorithms are applied to the generated training dataset and evaluated for their performance. Metrics such as accuracy, precision, recall and F1-score to quantify the classification performance are commonly employed. Further, cross-validation can also be used to estimate the generalization ability of an algorithm across different data subsets and, in addition, the predicted two-dimensional coordinates can be compared with the actual coordinates to quantify the position accuracy. Here, the following metrics are used for comparison and evaluation of the selected machine learning algorithms: the mean absolute error (MAE), which is basically indicating the mean deviation on the x- and the y-axis in mm, the root mean square error (RMSE), which is the standard deviation of the residuals, the mean error distance, which is the mean Euclidean distance in mm between the predicted and the actual two-dimensional position and the classification accuracy (CA), which is the ratio of correct predictions to the total number of input samples. The corresponding equations are expressed as follows:

$$MAE = \frac{\sum_{i=1}^{n} |y_i - x_i|}{n}, \tag{1}$$

$$RMSE = \sqrt{\frac{\sum_{i=1}^{n} (y_i - x_i)}{n}}, \tag{2}$$

$$Mean\ Error\ Distance = \frac{\sum_{i=1}^{n} \sqrt{\left(x_{y_i} - x_{x_i}\right)^2 + \left(y_{y_i} - y_{x_i}\right)^2}}{n}, \tag{3}$$

$$CA = \frac{Number\ of\ correct\ predictions}{n}. \tag{4}$$

The predicted value for the i^{th} position in the training dataset is y_i and x_i refers to the actual value of this position. The total amount of observations in the dataset is specified by n. To test the algorithms on datasets with different size, reduced training sets are created from the primary dataset by considering only every 10^{th} row, resulting in 10 measurements per position and a total size of $n = 6250$ rows. In connection with the size of the dataset the hyperparameters of each supervised learning algorithm are tuned to produce the best results in terms of the metrics evaluated in the comparison. For the evaluation of the algorithms the Python packages scikit-learn (k-Nearest Neighbours, Random Forest and Decision Tree) and TensorFlow (Neural Network) are used.

Table 1 gives an overview and a comparison of the results obtained with four investigated supervised learning algorithms, k-NN, RF, ANN and Decision Tree. The above described metrics are calculated for each algorithm and for two sizes of the training dataset. The results show that k-NN and RF give the best results in terms of accuracy and error metrics. It can also be see that the size of the training dataset has a significant influence on the performance metrics. Considering the computational constraints for the implementation on a microcontroller, the k-NN algorithm offers some advantages over RF and is therefore selected for the two-dimensional positioning algorithm in this work.

D. K-NEAREST NEIGHBORS ALGORITHM APPROACH

In general, the k-NN algorithm is well-suited for microcontroller applications because it does not require extensive training or model parameters. Instead, it relies on the stored training dataset to make predictions. Furthermore, the k-NN algorithm can be implemented on a microcontroller in a straightforward manner, as it mainly involves distance calculations and voting. These operations are associated only with small computing efforts and can be performed efficiently on microcontroller hardware. Another advantage of k-NN is its ability to handle online learning, where new data can be incrementally added to the existing training dataset in the flash memory of the microcontroller. This capability is valuable in scenarios where real-time learning and adaptation are essential, e.g. in possible extensions for future applications.

The k-NN algorithm is a lazy, non-parametric learning algorithm that does not assume a specific data distribution. In supervised learning, labelled training data is essential for predicting the outcome of new samples. Once the model has been constructed, the k-NN algorithm permanently stores the training data in memory. When new feature data x become available, the goal of the k-NN algorithm is to identify the k nearest neighbors of x from the training data. This process allows a classification by the label of the input data x. The value of k represents a positive integer that determines the

number of nearest neighbors to be considered. For example, if $k = 1$, the input data x is assigned to the class of its single nearest neighbor. In the model used in this work three nearest neighbors are considered ($k = 3$).

For the implementation of the k-NN algorithm, the Euclidean distance function is used to calculate the distance between all data points. This distance is given by the following formula:

$$d(x, y) = \sqrt{\sum_{j=1}^{N}\sum_{i=1}^{m}\left(x_i - y_{j,i}\right)^2}. \tag{5}$$

Here the features data vector is represented by x_i and $y_{j,i}$ specifies the respective labelled training data point. The number of rows in the training dataset is N and m the quantity of features per row. The weighted k-NN algorithm adopts a strategy where the weights $w(x, y)$ assigned to neighbors are derived from the inverse of their distances to the query point, which is expressed as follows:

$$w(x, y) = \frac{1}{d(x, y)}. \tag{6}$$

Consequently, the corresponding weights are subject to variation as they are influenced by the relationship between the neighbors and the feature set x [87]. This approach is based on the understanding that closer neighbors have a greater similarity, thus a higher weight value to the query point and therefore also a higher influence on the prediction process. By summing up weights, the algorithm takes into account the relative importance of each neighbor, resulting in improved accuracy and performance. For given neighbors and weights the weighted k-NN rule assigns the feature set x to the class c that yields the highest sum of weights among its representatives within the neighborhood n_i, which is expressed as follows:

$$x \longleftarrow \arg\max_{c}\left[\sum_{i=1}^{k} w_{n_i} B_c(n_i)\right], \tag{7}$$

where

$$B_c(n_i) = \begin{cases} 1 & \text{if neighbor } n_i \in c \\ 0 & \text{otherwise} \end{cases} \tag{8}$$

represents a binary indicator function for the class c, in dependency of the nearest points in the training set [88]. By assigning weights to neighbors based on their distances, the algorithm can adaptively adjust their influence on the final prediction.

When implementing the weighted k-NN algorithm on a microcontroller, it is crucial to optimize the computational efficiency by considering the specific weighting function that best suits the problem at hand.

E. IMPLEMENTATION OF THE 2D-POSITIONING ALGORITHM

To deploy the positioning algorithm, the recorded training dataset is transferred to the non-volatile memory area of the microcontroller. For this purpose, the comma-separated dataset (CSV-file) is converted to corresponding C programming language source (.c) and header (.h) files by a Python script, where the data is stored in multi-dimensional arrays. Due to the fact, that the complete dataset consisting of $n = 62500$ rows and 5 columns would consume 625 kB of memory (2 bytes per 16-bit unsigned integer entry), the reduced dataset with $n = 6250$ rows is considered for the implementation of the algorithm. The pseudocode of the implemented algorithm is provided in Algorithm 1.

Algorithm 1 Proposed Two-Dimensional Positioning Classification Algorithm

```
Input: features x[0 ... m − 1]
Output: Predicted position label
begin
    for i = 0 to n do        // n = number of rows in dataset
        for j = 0 to m do        // m = number of feature columns
            Calculate euclidean distance d(x, y) between incoming data and training dataset, see (5)
            Calculate corresponding weights w(x, y), see (6)
        end
    end
    Sort results according calculated to weights
    Calculate sum of weights for the k nearest neighbours
    Compute the category (position), see (7)
    Return predicted label
end
```

Due to the size of the data set and the calculations required, one iteration for position determination takes approximately 200 ms, which is many times longer than the iteration of a measurement cycle (16 ms). This leads to the problem that the classification result is not available in real time after each measurement cycle. Therefore, the computation of the introduced algorithm is continuously interrupted by the measurement process to guarantee an up to date position analysis for the retroreflective foil.

The accuracy, stability and time complexity of the proposed algorithm heavily depend on the number of stored data points in the training data set, together with the noise that occurs in the data. As described, the size and the quality in terms of noise of the training dataset is fixed due to the amount of flash memory of the microcontroller and the hardware itself. Thus, the remaining parameter for the convergence of Algorithm 1 is the number of the nearest neighbors k, which was found to give an optimum accuracy when three nearest neighbors are considered.

VI. EVALUATION OF THE LEDPOS DEMONSTRATOR AND RESULTS

A test scenario is applied in analogy to the generation of training datasets to evaluate and validate the performance of

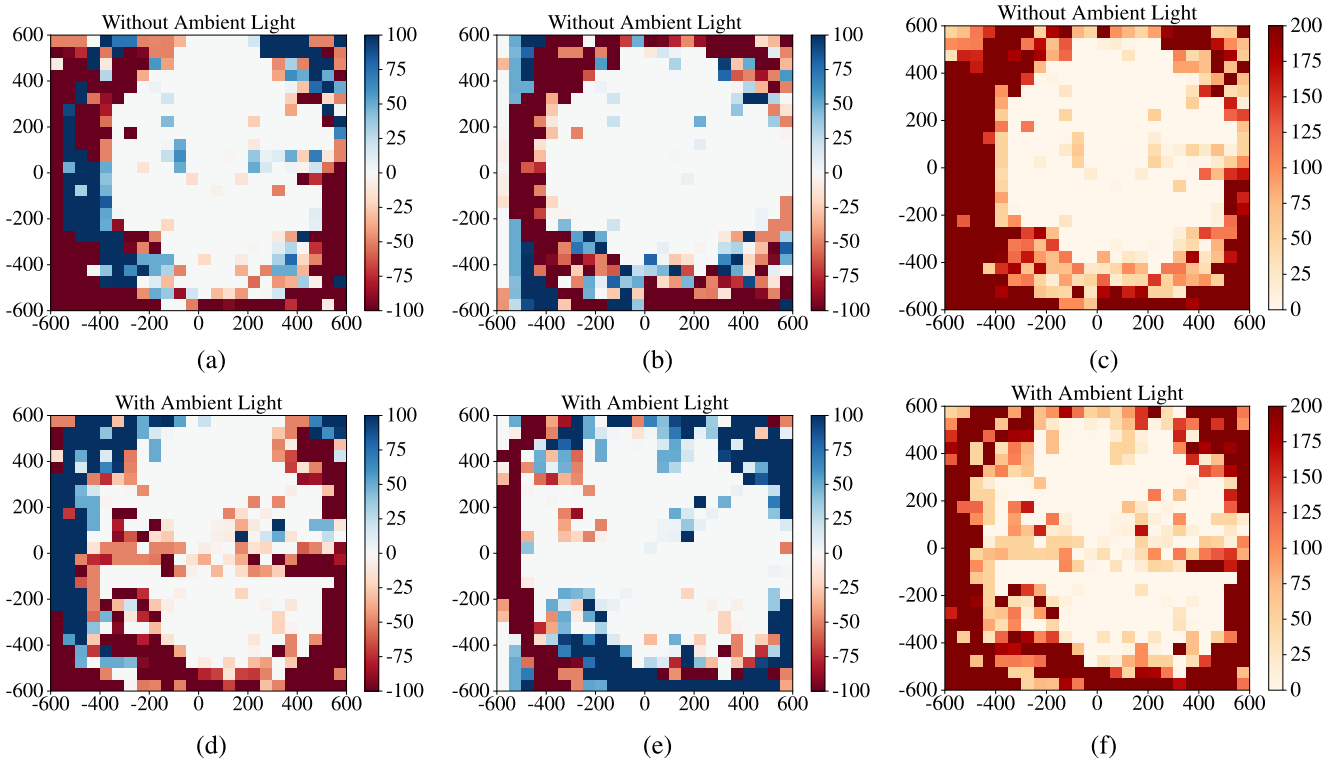

FIGURE 6. Mean error distances in x-axis (a) and (d), mean error distances in y-axis (b) and (e) and total mean error distances (c) and (f) obtained from test runs for system evaluation under two environmental conditions - without ambient light (top row) and with ambient light (bottom row). The axis dimensions as well as the mean error distances are given in mm.

TABLE 2. Mean error distances in dependency of the experimental area in m and the ambient conditions.

Conditions	Mean Absolute Error X-axis			Mean Absolute Error Y-axis			Mean Error Distance Total		
	1.2×1.2 m	0.8×0.8 m	0.4×0.4 m	1.2×1.2 m	0.8×0.8 m	0.4×0.4 m	1.2×1.2 m	0.8×0.8 m	0.4×0.4 m
without ambient light	156.2 mm	19 mm	4.9 mm	339 mm	18.4 mm	1.1 mm	441.2 mm	30 mm	5 mm
with ambient light	130.5 mm	23.7 mm	16.3 mm	132 mm	12.3 mm	5.6 mm	213 mm	29 mm	18 mm

the developed LEDPOS demonstrator system with the implemented two-dimensional positioning algorithm described in the previous section. The main goal is to quantify the accuracy for position determination of the retroreflective foil in the specified area of the experimental setup. Thus, the two-dimensional linear axis is used again to control x- and y-positions of the retroreflective foil and the reflected light was captured by the LEDPOS demonstrator and converted to input features for the positioning algorithm at each position of the foil. As before, the area for evaluation is 1.2 m × 1.2 m and is segmented with a 5 cm grid in both directions x and y. Test runs are performed by acquiring 50 predictions for each of the 625 positions, which then are averaged for each position and compared to the actual position obtained from the 2D linear stage control.

The positioning accuracy of the proposed LEDPOS demonstrator for 2D indoor positioning via BVLP is evaluated for two controlled conditions. The first scenario is related to a dark environment, i.e. without any ambient light sources such as the installed laboratory room lighting or daylight entering through the windows when the blinds are open. In this case, the only illumination in the test room comes from the LEDs of the LEDPOS demonstrator itself (3 LEDs used alternately for lighting, see Section IV-C). To evaluate the performance of the LEDPOS system in combination with the interference of additional light sources, in the second scenario the fluorescent room lights in the laboratory are switched on in addition to the LEDs of the demonstrator system. The illuminance determined in the center of the experimental area for these two situations is 82 lx (“without ambient light”) and 260 lx (“with ambient light”) respectively. The illuminance distribution for the “without ambient light” scenario in the total experimental area can be estimated from the simulation result shown in Fig. 5. Please note for comparison that for office workplaces an illuminance from 300 lx to 500 lx is required.

Fig. 6 visualizes the total mean error distance as well as the mean error distances for the two directions of the linear stage at every position in the test area. This summarizes the results from the performed test runs of the system and the outcome is compared for both tested ambient light conditions. The results show that the position of the retroreflective foil can be predicted with high accuracy in the center of the experimental area (white spots). Without ambient light the total mean error distance is in the range of 5 mm in the area of 0.4 m × 0.4 m and 30 mm in an area of approximately 0.8 m × 0.8 m. These areas are also indicated in Fig. 5 and it can be seen that high positioning accuracies match pretty well with areas of high illuminance as determined from the light simulations. Outside the center area, the accuracy of the two-dimensional position classification decreases, which can be related to the decreasing illuminance and the associated decrease in the light intensity reflected from the retroreflective foil towards the sensing LED of the LEDPOS demonstrator at the ceiling. This decreased reflected light intensity in the outer regions results in a low SNR and therefore also the signal variation of the raw data and the associated variation of features at different positions becomes too small for highly accurate predictions by the positioning algorithm. This demonstrates the limitations of the proposed LEDPOS system with its implemented machine learning algorithm for on the edge calculations on a microcontroller. Small sensor signals when using the LED illumination for sensing in combination with thermal variations and hence an increased noise between several test runs prevent high accurate position determination in areas with low illuminance. In comparison, when using the same algorithm on a standard PC with much higher computing power and memory compared to the employed microcontroller, larger training datasets could be used for example to cope with low prediction accuracies in areas with low illuminance. However, it is pointed out that there is still room for improvement by increasing the light intensity of the LEDPOS demonstrator itself, as the illumination levels applied are far below the requirements for workspaces (see above).

Finally, Table 2 summarizes some numerical results for the mean error distances evaluated for three different sizes of the experimental area and for the two environmental conditions with and without ambient light. Three conclusions are drawn from these results:

1) Position determination is performed with high accuracy in the range of several mm by the proposed LEDPOS demonstrator with implemented on the edge calculation as long as there is sufficient illumination in the target area.
2) A decreasing positioning accuracy is related to vanishing feature differences caused by small sensor signals.
3) A comparison of the two environmental conditions shows that the additional ambient light on the one hand improves the total mean error distance for the overall experimental target area of 1.2 m × 1.2 m, but on the other hand decreases the high position accuracy in the center area of 0.4 m × 0.4 m (for the area of 0.8 m × 0.8 m the total mean error distance is more or less the same for both conditions).

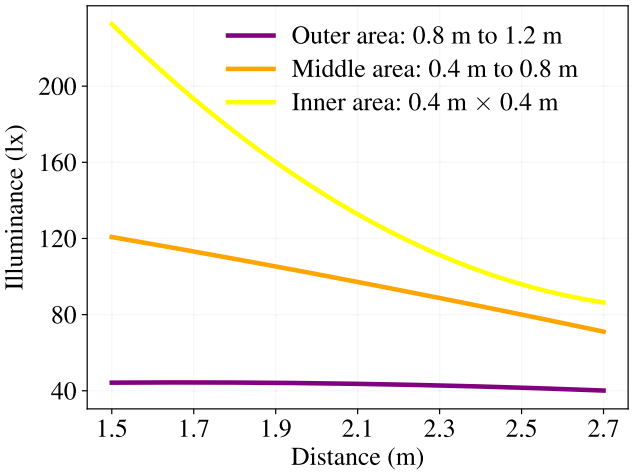

FIGURE 7. Simulated illuminance distribution (without ambient light) for three areas in the experimental plane as a function of the distance between the LEDPOS system and the experimental plane.

The performance of the LEDPOS demonstrator is further investigated for varying distances between the system and the retroreflective foil which refers to the target plane of positioning. For this purpose, the illuminance of the LEDPOS demonstrator is simulated for several planes at different distances from the system, similar to Fig. 5 which refers to a distance of 2.7 m. Furthermore, the resulting illuminance is examined separately in three areas of the experimental plane (see also Fig. 5) according to the analysis of the mean error distances in Table 2. The results are summarized in Fig. 7, which shows the effect of varying distances between the LEDPOS luminaire and the respective experimental plane under consideration. It can be seen that reducing the distance from the ceiling height of 2.7 m to smaller distances significantly increases the illuminance in the inner area of the experimental plane and moderately in the intermediate area. In contrast, the increase in illuminance in the outer area was found to be negligible under the given conditions of the setup. With regard to the mean error distances of the positioning algorithm, it is therefore to be expected that the positioning accuracy will neither improve for the outer area, as the illumination level there is more or less unchanged at a low level, nor for the inner area, where the positioning accuracy is already high and is limited by other restrictions of the system. Only for the intermediate area of the experimental plane it is to be expected that the positioning accuracy will increase with smaller distances between the retroreflective foil and the LEDPOS system.

VII. DISCUSSION AND FUTURE WORK

In general, the proposed LEDPOS demonstrator successfully exploits the capability of LEDs used as sensors, allowing simultaneous measurements of reflected light while provid-

ing flicker-free illumination with standard white-light LEDs. Based on this and the method of BVLP, a device-free and efficient two-dimensional positioning in indoor environments is demonstrated. Signal processing algorithms and machine learning techniques are implemented on a microcontroller of the demonstrator resulting in a self-contained, reliable system with a high positioning accuracy. The mean error distance in a real world arrangement is demonstrated to be as low as 5 mm as long as there is sufficient illuminance in the target area.

So far, a number of challenges regarding practical deployment have not been addressed, such as permanently changing light conditions, disturbing reflections and interferences, light blockages, or tilted conditions of the retroreflective foil with moving objects. However, it is assumed that many of these issues can only be solved for a very specific environment, whereas the aim of the present work is to demonstrate a general approach for indoor positioning by VLP. To sketch the envisaged solution in more detail, one can think of automated guided vehicles in logistics, for instance, where it does not represent a restriction that a retroreflective foils is attached to this vehicle in a fixed horizontal orientation and a fixed height. In contrast to indoor positioning by geometry based approaches like RSS or AoA, where certainly more than one lighting point is needed, the proposed LEDPOS system can already realize indoor positioning within a certain area covered by the illumination field of one system (''VLP unit cell''). It is expected that the combination of a passive retroreflective foil on the object of interest with only one ceiling mounted LEDPOS system can be implemented with low deployment costs. Another advantage of the proposed approach is that the field of view for the illumination and for the sensing functionality in such a ''VLP unit cell'' inherently matches for all designs of the illumination optics, as the LEDs are employed for both sensing and illumination. Contrary, it might be difficult to realize this by independent components in a miniaturized manner (e.g. separate photodiode for sensing in addition to LED illumination).

Concerning scalability, it is even possible to imagine using the current version of the LEDPOS demonstrator for larger indoor spaces than were investigated in the current experimental setup simply by using additional LEDPOS systems. However, optimizing the system and the connection of several luminaires for positioning are aspects that need to be considered in future work. Furthermore, the system's sensitivity to ambient light conditions, as indicated by the comparison of the two ambient lighting situations studied, remains one of the major challenges for future investigations. The proposed approach of using a retroreflective foil, which in principle reflects the incident light back in the same direction, reduces the effects of disturbances from unwanted reflections or changes in ambient light, but of course cannot eliminate all influences. Fluctuations in the ambient light levels can cause variations in the measured signals and, thus potentially affect the position accuracy. Future studies need to address this issue and explore techniques to mitigate the impact of ambient light variations on the system performance. Nevertheless, the results obtained demonstrate that our approach can be combined with other ambient light sources and show that it is possible to retrofit an LED-sensing luminaire to monitor a specific area of a room without having to adapt or modify the existing room lighting.

The position accuracy achieved in this work is considered to enable several practical implementations of indoor positioning applications. The LEDPOS system, used in environmental conditions with constant illumination, can improve or facilitate functionalities and processes. For example, in industrial environments, the system is able to estimate and track the two-dimensional position of objects such as autonomous robots to which a retroreflective foil can be easily attached. Other applications are related to detect trespassing of humans or robots in defined safety zones and in general, indoor positioning is expected to become of increasing importance for areas such as warehouse automation, collaborative robotics, or any industrial processes, where precise localization is crucial for efficient and safe operations.

VIII. CONCLUSION

The hardware design, the positioning algorithm, a strategy for implementation and the experimental evaluation in a real-world setting are presented for the LEDPOS demonstrator, which uses LEDs as sensors and an on-the-edge algorithm to implement an indoor positioning system based on BVLP. It is demonstrated that the two-dimensional position of a retroreflective foil at the floor can be calculated from reflections backscattered to the ceiling mounted device with an average distance error being as low as 5 mm with respect to the actual position, while providing unimpaired illumination with standard white-light LEDs.

Some potential industrial applications are outlined, where high precision indoor positioning can leverage the efficiency and facilitate new functionalities and processes. As the proposed demonstrator can be combined with the existing lighting infrastructure and the positioning algorithm is based on non-parametric machine learning, the system can be used independently and implemented with low installation effort. In addition, the use of LEDs as light sources and sensors enables very compact luminaire sizes, since no additional photosensitive devices have to be integrated, thus retrofitting existing luminaires can be achieved in a straightforward manner.

Future work needs to address the challenges considered with varying ambient light conditions and strategies to combine several systems for a deployment in large areas.

REFERENCES

[1] D. Feezell and S. Nakamura, ''Invention, development, and status of the blue light-emitting diode, the enabler of solid-state lighting,'' *Comp. Rendus Physique*, vol. 19, no. 3, pp. 113–133, 2018. [Online]. Available: https://www.sciencedirect.com/science/article/pii/S163107051730124X

[2] T.-C. Yu, W.-T. Huang, W.-B. Lee, C.-W. Chow, S.-W. Chang, and H.-C. Kuo, "Visible light communication system technology review: Devices, architectures, and applications," *Crystals*, vol. 11, no. 9, p. 1098, Sep. 2021. [Online]. Available: https://www.mdpi.com/2073-4352/11/9/1098

[3] S. S. Oyewobi, K. Djouani, and A. M. Kurien, "Visible light communications for Internet of Things: Prospects and approaches, challenges, solutions and future directions," *Technologies*, vol. 10, no. 1, p. 28, Feb. 2022. [Online]. Available: https://www.mdpi.com/2227-7080/10/1/28

[4] N. Chaudhary, L. N. Alves, and Z. Ghassemblooy, "Current trends on visible light positioning techniques," in *Proc. 2nd West Asian Colloq. Opt. Wireless Commun. (WACOWC)*, Apr. 2019, pp. 100–105.

[5] W. Gu, M. Aminikashani, P. Deng, and M. Kavehrad, "Impact of multipath reflections on the performance of indoor visible light positioning systems," *J. Lightw. Technol.*, vol. 34, no. 10, pp. 2578–2587, May 2016.

[6] P. Lou, H. Zhang, X. Zhang, M. Yao, and Z. Xu, "Fundamental analysis for indoor visible light positioning system," in *Proc. 1st IEEE Int. Conf. Commun. China Workshops (ICCC)*, Aug. 2012, pp. 59–63.

[7] S. De Lausnay, L. De Strycker, J.-P. Goemaere, B. Nauwelaers, and N. Stevens, "A survey on multiple access visible light positioning," in *Proc. IEEE Int. Conf. Emerg. Technol. Innov. Business Practices Transformation Societies (EmergiTech)*, Aug. 2016, pp. 38–42.

[8] V. P. Rekkas, L. A. Iliadis, S. P. Sotiroudis, A. D. Boursianis, P. Sarigiannidis, D. Plets, W. Joseph, S. Wan, C. G. Christodoulou, G. K. Karagiannidis, and S. K. Goudos, "Artificial intelligence in visible light positioning for indoor IoT: A methodological review," *IEEE Open J. Commun. Soc.*, vol. 4, pp. 2838–2869, 2023.

[9] P. H. Pathak, X. Feng, P. Hu, and P. Mohapatra, "Visible light communication, networking, and sensing: A survey, potential and challenges," *IEEE Commun. Surveys Tuts.*, vol. 17, no. 4, pp. 2047–2077, 4th Quart., 2015.

[10] C. Liang, J. Li, S. Liu, F. Yang, Y. Dong, J. Song, X.-P. Zhang, and W. Ding, "Integrated sensing, lighting and communication based on visible light communication: A review," *Digit. Signal Process.*, vol. 145, Feb. 2024, Art. no. 104340. [Online]. Available: https://www.sciencedirect.com/science/article/pii/S1051200423004359

[11] K. Madane, A. P. Weiss, S. Schantl, E. Leitgeb, and F. P. Wenzl, "Machine learning assisted visible light sensing of the rotation of a robotic arm," *IEEE Access*, vol. 9, pp. 130721–130736, 2021.

[12] C. Fragner, A. P. Weiss, F. P. Wenzl, and E. Leitgeb, "Integrated sensing and communication in the visible spectral range: A novel closed loop controller," in *Proc. Int. Conf. Broadband Commun. Next Gener. Netw. Multimedia Appl. (CoBCom)*, Jul. 2022, pp. 1–7.

[13] A. P. Weiss, C. Fragner, and F. P. Wenzl, "A novel approach for human-system interaction by visible light sensing based wrist posture and rotation determination," in *Proc. 14th Int. Conf. Hum. Syst. Interact. (HSI)*, Jul. 2021, pp. 1–6.

[14] O. E. Ouahabi, C. Fragner, A. P. Weiss, and E. Leitgeb, "Occupancy determination by backscattered visible light sensing," in *Proc. 46th MIPRO ICT Electron. Conv. (MIPRO)*, May 2023, pp. 280–285.

[15] Z. Salem, C. Krutzler, C. Fragner, and A. P. Weiss, "Visible light technologies for the industrial Internet of Things," in *Proc. 17th Int. Conf. Telecommun. (ConTEL)*, Jul. 2023, pp. 1–8.

[16] C. Fragner, C. Krutzler, A. P. Weiss, and E. Leitgeb, "Visual light sensing for IoT sensor networks: A use case for monitoring rotating shaft conditions in industrial applications," in *Proc. 17th Int. Conf. Telecommun. (ConTEL)*, Jul. 2023, pp. 1–7.

[17] A. Basiri, E. S. Lohan, T. Moore, A. Winstanley, P. Peltola, C. Hill, P. Amirian, and P. Figueiredo e Silva, "Indoor location based services challenges, requirements and usability of current solutions," *Comput. Sci. Rev.*, vol. 24, pp. 1–12, May 2017. [Online]. Available: https://www.sciencedirect.com/science/article/pii/S1574013716301782

[18] E. W. Lam and T. D. C. Little, "Visible light positioning for location-based services in industry 4.0," in *Proc. 16th Int. Symp. Wireless Commun. Syst. (ISWCS)*, Aug. 2019, pp. 345–350.

[19] F. M. Mims, "Sun photometer with light-emitting diodes as spectrally selective detectors," *Appl. Opt.*, vol. 31, no. 33, p. 6965, Nov. 1992.

[20] E. Miyazaki, S. Itami, and T. Araki, "Using a light-emitting diode as a high-speed, wavelength selective photodetector," *Rev. Sci. Instrum.*, vol. 69, no. 11, pp. 3751–3754, Nov. 1998.

[21] E. Kaplan and C. J. Hegarty, *Understanding GPS/GNSS: Principles and Applications*, 3rd ed. Norwood, MA, USA: Artech House, 2017.

[22] M. B. Kjærgaard, H. Blunck, T. Godsk, T. Toftkjær, D. L. Christensen, and K. Grønbæk, "Indoor positioning using GPS revisited," in *Pervasive Computing*, P. Floréen, A. Krüger, and M. Spasojevic, Eds. Berlin, Germany: Springer, 2010, pp. 38–56.

[23] R. Brena, J. García-Vázquez, C. Galván Tejada, D. Munoz, C. Vargas-Rosales, J. Fangmeyer Jr, and A. Palma, "Evolution of indoor positioning technologies: A survey," *J. Sensors*, vol. 2017, Mar. 2017, Art. no. 2630413.

[24] H. Liu, H. Darabi, P. Banerjee, and J. Liu, "Survey of wireless indoor positioning techniques and systems," *IEEE Trans. Syst., Man, Cybern., C (Appl. Rev.)*, vol. 37, no. 6, pp. 1067–1080, Nov. 2007, doi: 10.1109/TSMCC.2007.905750.

[25] T. Simelane, T. N. Mathaba, and T. O. Otunniyi, "A review paper: Indoor positioning systems using radio frequency technology," in *Proc. Int. Conf. Elect., Comput. Energy Technol. (ICECET)*, Nov. 2023, pp. 1–7.

[26] F. Liu, J. Liu, Y. Yin, W. Wang, D. Hu, P. Chen, and Q. Niu, "Survey on WiFi-based indoor positioning techniques," *IET Commun.*, vol. 14, no. 9, pp. 1372–1383, Jun. 2020.

[27] S. Shang and L. Wang, "Overview of WiFi fingerprinting-based indoor positioning," *IET Commun.*, vol. 16, no. 7, pp. 725–733, Apr. 2022.

[28] L. P. Fraile and C. Koulamas, "Design and evaluation of an indoor positioning system based on mobile devices," in *Proc. 11th Medit. Conf. Embedded Comput. (MECO)*, Jun. 2022, pp. 1–6.

[29] A. Alarifi, A. Al-Salman, M. Alsaleh, A. Alnafessah, S. Al-Hadhrami, M. Al-Ammar, and H. Al-Khalifa, "Ultra wideband indoor positioning technologies: Analysis and recent advances," *Sensors*, vol. 16, no. 5, p. 707, May 2016. [Online]. Available: https://www.mdpi.com/1424-8220/16/5/707

[30] J. Qu, "A review of UWB indoor positioning," in *Proc. J. Phys., Conf.*, Dec. 2023, vol. 2669, no. 1, Art. no. 012003, doi: 10.1088/1742-6596/2669/1/012003.

[31] M. Hazas and A. Hopper, "Broadband ultrasonic location systems for improved indoor positioning," *IEEE Trans. Mobile Comput.*, vol. 5, no. 5, pp. 536–547, May 2006.

[32] A. R. Jimenez Ruiz, F. Seco Granja, J. C. Prieto Honorato, and J. I. Guevara Rosas, "Accurate pedestrian indoor navigation by tightly coupling foot-mounted IMU and RFID measurements," *IEEE Trans. Instrum. Meas.*, vol. 61, no. 1, pp. 178–189, Jan. 2012.

[33] F. Bernardini, A. Buffi, D. Fontanelli, D. Macii, V. Magnago, M. Marracci, A. Motroni, P. Nepa, and B. Tellini, "Robot-based indoor positioning of UHF-RFID tags: The SAR method with multiple trajectories," *IEEE Trans. Instrum. Meas.*, vol. 70, 2021, Art. no. 8001415.

[34] Z. Wei, J. Chen, H. Tang, and H. Zhang, "RSSI-based location fingerprint method for RFID indoor positioning: A review," *Nondestruct. Test. Eval.*, vol. 39, no. 1, pp. 3–31, 2023, doi: 10.1080/10589759.2023.2253493.

[35] Y. Zhuang, L. Hua, L. Qi, J. Yang, P. Cao, Y. Cao, Y. Wu, J. Thompson, and H. Haas, "A survey of positioning systems using visible LED lights," *IEEE Commun. Surveys Tuts.*, vol. 20, no. 3, pp. 1963–1988, 3rd Quart., 2018.

[36] A. B. M. M. Rahman, T. Li, and Y. Wang, "Recent advances in indoor localization via visible lights: A survey," *Sensors*, vol. 20, no. 5, p. 1382, Mar. 2020. [Online]. Available: https://www.mdpi.com/1424-8220/20/5/1382

[37] J. Singh and U. Raza, "Passive visible light positioning systems: An overview," in *Proc. Workshop Light IoT*, New York, NY, USA, 2020, pp. 48–53, doi: 10.1145/3412449.3412553.

[38] M. Afzalan and F. Jazizadeh, "Indoor positioning based on visible light communication: A performance-based survey of real-world prototypes," *ACM Comput. Surv.*, vol. 52, no. 2, p. 35, May 2019, doi: 10.1145/3299769.

[39] J. Armstrong, Y. A. Sekercioglu, and A. Neild, "Visible light positioning: A roadmap for international standardization," *IEEE Commun. Mag.*, vol. 51, no. 12, pp. 68–73, Dec. 2013.

[40] M. O'Toole and D. Diamond, "Absorbance based light emitting diode optical sensors and sensing devices," *Sensors*, vol. 8, no. 4, pp. 2453–2479, Apr. 2008. [Online]. Available: https://www.mdpi.com/1424-8220/8/4/2453

[41] G. Schirripa Spagnolo, F. Leccese, and M. Leccisi, "LED as transmitter and receiver of light: A simple tool to demonstration photoelectric effect," *Crystals*, vol. 9, no. 10, p. 531, Oct. 2019.

[42] K. Reynolds, J. De Kock, L. Tarassenko, and J. Moyle, "Temperature dependence of LED and its theoretical effect on pulse oximetry," *Brit. J. Anaesthesia*, vol. 67, no. 5, pp. 638–643, 1991. [Online]. Available: https://www.sciencedirect.com/science/article/pii/S0007091217478913

[43] Y. Yang, J. Hao, J. Luo, and S. J. Pan, "CeilingSee: Device-free occupancy inference through lighting infrastructure based LED sensing," in *Proc. IEEE Int. Conf. Pervasive Comput. Commun. (PerCom)*, Mar. 2017, pp. 247–256.

[44] F. Sakr, F. Bellotti, R. Berta, and A. De Gloria, "Machine learning on mainstream microcontrollers," *Sensors*, vol. 20, no. 9, p. 2638, May 2020. [Online]. Available: https://www.mdpi.com/1424-8220/20/9/2638

[45] S. S. Saha, S. S. Sandha, and M. Srivastava, "Machine learning for microcontroller-class hardware: A review," *IEEE Sensors J.*, vol. 22, no. 22, pp. 21362–21390, Nov. 2022.

[46] M. Kowalczyk and J. Siuzdak, "Photo-reception properties of common LEDs," *Opto-Electron. Rev.*, vol. 25, no. 3, pp. 222–228, Sep. 2017.

[47] J. Sticklus, P. A. Hoeher, and M. Hieronymi, "Experimental characterization of single-color power LEDs used as photodetectors," *Sensors*, vol. 20, no. 18, p. 5200, Sep. 2020.

[48] M. Galal, W. P. Ng, R. Binns, and A. A. El Aziz, "Characterization of RGB LEDs as emitter and photodetector for LED-to-LED communication," in *Proc. 12th Int. Symp. Commun. Syst., Netw. Digit. Signal Process. (CSNDSP)*, Jul. 2020, pp. 1–6.

[49] G. Stepniak, M. Kowalczyk, L. Maksymiuk, and J. Siuzdak, "Transmission beyond 100 Mbit/s using LED both as a transmitter and receiver," *IEEE Photon. Technol. Lett.*, vol. 27, no. 19, pp. 2067–2070, Oct. 2015.

[50] D. Milovancev, N. Vokic, H. Hübel, and B. Schrenk, "Gb/s visible light communication with low-cost receiver based on single-color LED," *J. Lightw. Technol.*, vol. 38, no. 12, pp. 3305–3314, Jun. 2020.

[51] S. Li, B. Huang, and Z. Xu, "Experimental MIMO VLC systems using tricolor LED transmitters and receivers," in *Proc. IEEE Globecom Workshops (GC Wkshps)*, Dec. 2017, pp. 1–6.

[52] P. Dietz, W. Yerazunis, and D. Leigh, "Very low-cost sensing and communication using bidirectional LEDs," in *Proc. Int. Conf. Ubiquitous Comput.*, Oct. 2003, pp. 175–191.

[53] L. Incipini, A. Belli, L. Palma, M. Ballicchia, and P. Pierleoni, "Sensing light with LEDs: Performance evaluation for IoT applications," *J. Imag.*, vol. 3, no. 4, p. 50, Nov. 2017.

[54] K. Lau, S. Baldwin, R. Shepherd, P. Dietz, W. Yerzunis, and D. Diamond, "Novel fused-LEDs devices as optical sensors for colorimetric analysis," *Talanta*, vol. 63, pp. 167–173, May 2004.

[55] M. O'Toole, R. Shepherd, K.-T. Lau, and D. Diamond, "Detection of nitrite by flow injection analysis using a novel paired emitter-detector diode (PEDD) as a photometric detector," in *Advanced Environmental, Chemical, and Biological Sensing Technologies V* (International Society for Optics and Photonics), vol. 6755, T. Vo-Dinh, R. A. Lieberman, and G. Gauglitz, Eds. Bellingham, WA, USA: SPIE, 2007, Art. no. 67550P, doi: 10.1117/12.737791.

[56] M. O'Toole, K. Lau, R. Shepherd, C. Slater, and D. Diamond, "Determination of phosphate using a highly sensitive paired emitter–detector diode photometric flow detector," *Analytica Chim. Acta*, vol. 597, pp. 290–294, Aug. 2007.

[57] B. Raychaudhuri and C. Sen, "Light emitting diode as sensor for miniature multispectral radiometer," *Appl. Phys. B, Lasers Opt.*, vol. 95, pp. 141–144, Apr. 2009.

[58] S. Li and A. Pandharipande, "LED-based color sensing and control," *IEEE Sensors J.*, vol. 15, no. 11, pp. 6116–6124, Nov. 2015.

[59] M. S. Mir, B. Majlesein, B. G. Guzman, J. Rufo, and D. Giustiniano, "RGB LED bulbs for communication, harvesting and sensing," in *Proc. IEEE Int. Conf. Pervasive Comput. Commun. (PerCom)*, Mar. 2022, pp. 180–186.

[60] Z. Chen, Y. Yang, C. Jiang, J. Hao, and L. Zhang, "Light sensor based occupancy estimation via Bayes filter with neural networks," *IEEE Trans. Ind. Electron.*, vol. 67, no. 7, pp. 5787–5797, Jul. 2020.

[61] M. F. Keskin, A. D. Sezer, and S. Gezici, "Localization via visible light systems," *Proc. IEEE*, vol. 106, no. 6, pp. 1063–1088, Jun. 2018.

[62] H. Obeidat, W. Shuaieb, O. Obeidat, and R. Abd-Alhameed, "A review of indoor localization techniques and wireless technologies," *Wireless Pers. Commun.*, vol. 119, no. 1, pp. 289–327, Jul. 2021.

[63] Z. Zhu, Y. Yang, M. Chen, C. Guo, J. Cheng, and S. Cui, "A survey on indoor visible light positioning systems: Fundamentals, applications, and challenges," 2024, *arXiv:2401.13893*.

[64] T. Wenge, M. T. Chew, F. Alam, and G. S. Gupta, "Implementation of a visible light based indoor localization system," in *Proc. IEEE Sensors Appl. Symp. (SAS)*, Mar. 2018, pp. 1–6.

[65] Y. Almadani, M. Ijaz, W. Joseph, S. Bastiaens, S. Rajbhandari, B. Adebisi, and D. Plets, "A novel 3D visible light positioning method using received signal strength for industrial applications," *Electronics*, vol. 8, no. 11, p. 1311, Nov. 2019.

[66] C. Wang, L. Wang, X. Chi, S. Liu, W. Shi, and J. Deng, "The research of indoor positioning based on visible light communication," *China Commun.*, vol. 12, no. 8, pp. 85–92, Aug. 2015.

[67] S.-H. Yang, H.-S. Kim, Y.-H. Son, and S.-K. Han, "Three-dimensional visible light indoor localization using AOA and RSS with multiple optical receivers," *J. Lightw. Technol.*, vol. 32, no. 14, pp. 2480–2485, Jul. 2014.

[68] G. M. Mendoza-Silva, J. Torres-Sospedra, and J. Huerta, "A meta-review of indoor positioning systems," *Sensors*, vol. 19, no. 20, p. 4507, Oct. 2019. [Online]. Available: https://www.mdpi.com/1424-8220/19/20/4507

[69] C.-Y. Hong, Y.-C. Wu, Y. Liu, C.-W. Chow, C.-H. Yeh, K.-L. Hsu, D.-C. Lin, X.-L. Liao, K.-H. Lin, and Y.-Y. Chen, "Angle-of-arrival (AOA) visible light positioning (VLP) system using solar cells with third-order regression and ridge regression algorithms," *IEEE Photon. J.*, vol. 12, no. 3, pp. 1–5, Jun. 2020.

[70] C. Xie, W. Guan, Y. Wu, L. Fang, and Y. Cai, "The LED-ID detection and recognition method based on visible light positioning using proximity method," *IEEE Photon. J.*, vol. 10, no. 2, pp. 1–16, Apr. 2018.

[71] N. Chaudhary, L. N. Alves, and Z. Ghassemlooy, "Impact of transmitter positioning and orientation uncertainty on RSS-based visible light positioning accuracy," *Sensors*, vol. 21, no. 9, p. 3044, Apr. 2021. [Online]. Available: https://www.mdpi.com/1424-8220/21/9/3044

[72] T. Akiyama, M. Sugimoto, and H. Hashizume, "Time-of-arrival-based smartphone localization using visible light communication," in *Proc. Int. Conf. Indoor Positioning Indoor Navigat. (IPIN)*, Sep. 2017, pp. 1–7.

[73] I. M. Abou-Shehada, A. F. AlMuallim, A. K. AlFaqeh, A. H. Muqaibel, K.-H. Park, and M.-S. Alouini, "Accurate indoor visible light positioning using a modified pathloss model with sparse fingerprints," *J. Lightw. Technol.*, vol. 39, no. 20, pp. 6487–6497, Oct. 2021.

[74] Y. Chen, W. Guan, J. Li, and H. Song, "Indoor real-time 3-D visible light positioning system using fingerprinting and extreme learning machine," *IEEE Access*, vol. 8, pp. 13875–13886, 2020.

[75] V. Nguyen, M. Ibrahim, S. Rupavatharam, M. Jawahar, M. Gruteser, and R. Howard, "Eyelight: Light-and-shadow-based occupancy estimation and room activity recognition," in *Proc. IEEE Conf. Comput. Commun. (INFOCOM)*, Apr. 2018, pp. 351–359.

[76] N. Faulkner, F. Alam, M. Legg, and S. Demidenko, "Watchers on the wall: Passive visible light-based positioning and tracking with embedded light-sensors on the wall," *IEEE Trans. Instrum. Meas.*, vol. 69, no. 5, pp. 2522–2532, May 2020.

[77] S. Zhang, K. Liu, Y. Ma, X. Huang, X. Gong, and Y. Zhang, "An accurate geometrical multi-target device-free localization method using light sensors," *IEEE Sensors J.*, vol. 18, no. 18, pp. 7619–7632, Sep. 2018.

[78] D. Konings, N. Faulkner, F. Alam, E. M.-K. Lai, and S. Demidenko, "FieldLight: Device-free indoor human localization using passive visible light positioning and artificial potential fields," *IEEE Sensors J.*, vol. 20, no. 2, pp. 1054–1066, Jan. 2020.

[79] C. Fragner, A. P. Weiss, and F. P. Wenzl, "Backscattered visual light positioning using LED sensing in combination with edge computing based artificial neural network classification," in *Proc. Smart Syst. Integr. (SSI)*, Apr. 2022, pp. 1–6.

[80] R. I. AG. (2023). *Reluxdesktop—Free Software for Professional Lighting Planning*. [Online]. Available: https://relux.com/en/relux-desktop.html

[81] S. Xu, C.-C. Chen, Y. Wu, X. Wang, and F. Wei, "Adaptive residual weighted K-nearest neighbor fingerprint positioning algorithm based on visible light communication," *Sensors*, vol. 20, no. 16, p. 4432, Aug. 2020. [Online]. Available: https://www.mdpi.com/1424-8220/20/16/4432

[82] H. Q. Tran and C. Ha, "Machine learning in indoor visible light positioning systems: A review," *Neurocomputing*, vol. 491, pp. 117–131, Jun. 2022. [Online]. Available: https://www.sciencedirect.com/science/article/pii/S092523122200306X

[83] L. Breiman, "Random forests," *Mach. Learn.*, vol. 45, no. 1, pp. 5–32, Oct. 2001, doi: 10.1023/A:1010933404324.

[84] S. Suthaharan, *Support Vector Machine*. Boston, MA, USA: Springer, 2016, pp. 207–235, doi: 10.1007/978-1-4899-7641-3_9.

[85] O. Kramer, *K-Nearest Neighbors*. Berlin, Germany: Springer, 2013, pp. 13–23, doi: 10.1007/978-3-642-38652-7_2.

[86] J. J. Hopfield, "Artificial neural networks," *IEEE Circuits Devices Mag.*, vol. D-4, no. 5, pp. 3–10, Sep. 1988.

[87] S. A. Dudani, "The distance-weighted K-nearest-neighbor rule," *IEEE Trans. Syst., Man, Cybern.*, vol. SMC-6, no. 4, pp. 325–327, Apr. 1976.
[88] M. Bicego and M. Loog, "Weighted K-nearest neighbor revisited," in *Proc. 23rd Int. Conf. Pattern Recognit. (ICPR)*, Dec. 2016, pp. 1642–1647.

CHRISTIAN FRAGNER received the B.Sc. and M.Sc. degrees in electronics and computer engineering from the University of Applied Sciences FH Joanneum, Graz, Austria, in 2017 and 2019, respectively. He is currently pursuing the Ph.D. degree in information and communications engineering with Technical University Graz.

After several years in the lighting industry, he joined JOANNEUM RESEARCH, in 2020, where he is a Scientist in the field of embedded computing and smart connected lighting.

CHRISTIAN KRUTZLER received the Ph.D. degree in technical physics from Vienna University of Technology, in 2006.

After working for more than 15 years in research for optical methods and sensor technologies and in optical design for applications in medical technology, he has been with the Research Group Smart Connected Lighting, JOANNEUM RESEARCH, since 2022, on technologies for visible light, such as visible light sensing and visible light positioning.

ANDREAS PETER WEISS received the master's degree in telematics from Graz University of Technology, in 2008, and the Ph.D. degree from the Alpen Adria University of Klagenfurt, in 2012.

From 2012 to 2018, he worked in the field of research and development of digital circuit design, signal processing, and algorithm design. Since 2018, he has been a member with the Smart Connected Lighting Group, JOANNEUM RESEARCH Forschungsgesellschaft mbH, Pinkafeld, Austria. In 2022, he became the Group Leader. His research interests include visible light sensing, visible light positioning, sensors, sensor fusion, and algorithm design.

ERICH LEITGEB (Member, IEEE) received the master's degree from Graz University of Technology, in 1994, and the Ph.D. degree (Hons.), in February 1999.

From 1982 to 1984, he attended military service, including training to become an Officer for communications in Austrian Army. In 1994, he started research in optical communications with the Department of Communications and Wave Propagation, Graz University of Technology. Since January 2000, he has been the Project Leader of international research projects in the field of optical communications. Since 2011, he has been a Professor of optical communications and wireless applications with the Institute of Microwave and Photonic Engineering, Graz University of Technology. He is currently active as an Expert in military communications (current military rank: Lieutenant-Colonel). He has established and leads the Research Group for Optical Communications, Graz University of Technology. He joined several international projects (such as COST 270, the EU Project SatNEx and SatNEx 2, COST 291, COST IC0802, and IC1101, and he participates in MP1401, CA15127, and CA16220) and ESA projects in different functions. He is the author or coauthor of seven book chapters, more than 50 journal publications, 150 peer-reviewed conference papers, more than 45 invited talks, and more than 70 international scientific reports.